Predictive and therapeutic value of the ferroptosis gene CISD1 in non-small cell lung cancer

TAO WANG[1,2], XIAOYU XIAO[3], ZHE ZHANG[2] and XIANG LI[4]

[1]Department of Pathology, Shenyang KingMed Center for Clinical Laboratory Co., Ltd., Shenyang, Liaoning 110135, P.R. China;
[2]Department of Pathology, Shengjing Hospital of China Medical University, Shenyang, Liaoning 110801, P.R. China;
[3]Medical Laboratory College, Liaoning University of Traditional Chinese Medicine, Shenyang, Liaoning 116600, P.R. China;
[4]Department of Geriatrics, Central Hospital Affiliated to Shenyang Medical College, Shenyang, Liaoning 110075, P.R. China

Received September 29, 2024; Accepted January 17, 2025

DOI: 10.3892/ol.2025.14981

Abstract. The present study aimed to investigate the expression of ferroptosis genes in non-small cell lung cancer and their relationship with prognosis, and to analyze the relationship between ferroptosis genes and tumor immunity. To evaluate the expression levels of ferroptosis genes and their association with prognosis in lung adenocarcinoma (LUAD) and lung squamous cell carcinoma (LUSC), The Cancer Genome Atlas LUAD and LUSC data were downloaded, patient clinical information and ferroptosis gene expression profiles were extracted, and differential gene expression, survival and correlation analyses were performed using R. Using immune correlation analysis, the value of ferroptosis genes for immunotherapy was explored. The potential application of ferroptosis genes in immunotherapy was further validated by immunohistochemical staining. A number of ferroptosis-associated genes were differentially expressed in tumor tissues compared with in non-tumor tissues. CDGSH iron-sulfur domain-containing protein 1 (CISD1) was upregulated in both LUAD and LUSC tumor tissues, and was associated with tumor Tumor-Node-Metastasis stage. Notably, high levels of CISD1 in LUAD indicated a poor prognosis, and CISD1 was negatively correlated with $CD4^+$ T cells based on the immune score. Furthermore, CISD1 may be involved in pathways such as cellular response to hypoxia, DNA repair, extracellular matrix-related genes, epithelial-mesenchymal transition markers, oxidative phosphorylation and PI3K-AKT-mTOR pathway. Immunohistochemical staining indicated that CISD1 was highly expressed in LUAD tissues, it was associated with a poor prognosis of patients with LUAD, and it was negatively associated with CD4 and CD20. In conclusion, the ferroptosis gene CISD1 may be associated with the prognosis of LUAD, and high levels of CISD1 could indicate a shorter survival time. Furthermore, CISD1 has potential applications in immunotherapy. These findings may provide novel theoretical insights into the treatment of LUAD.

Correspondence to: Professor Xiang Li, Department of Geriatrics, Central Hospital Affiliated to Shenyang Medical College, 5 Nanqi West Road, Tiexi, Shenyang, Liaoning 110075, P.R. China
E-mail: 117107439@qq.com

Key words: ferroptosis, lung adenocarcinoma, CDGSH iron-sulfur domain-containing protein 1, prognosis, immune correlation

Introduction

The incidence and mortality rates of lung cancer are increasing every year (1), and lung cancer is one of the most important malignant tumors that threatens human health (2). Among lung cancer types, non-small cell lung cancer (NSCLC) is dominant, of which lung adenocarcinoma (LUAD) and lung squamous cell carcinoma (LUSC) are the main subtypes (3). Different chemotherapy regimens are required to treat different molecular subtypes; however, some patients will develop drug resistance or metastasis after treatment, which ultimately leads to adverse outcomes (4). The lives of patients may be prolonged and their quality of life improved by identifying novel indicators, designing new drugs and providing novel treatments for patients with drug resistance, poor prognosis or intolerance to some chemotherapeutic drugs.

Ferroptosis is an iron-dependent mode of cell death, which is characterized by a large iron-dependent accumulation of lethal lipid reactive oxygen species (ROS) (5,6). Numerous studies have focused on ferroptosis in the treatment of tumors. For example, in hepatocellular carcinoma, the induction of ferroptosis can lead to the infiltration and activation of $CD8^+$ T cells, this then leads to the upregulation of programmed death-ligand 1 in tumor cells (7). In breast cancer, the luminal androgen receptor (LAR) subtype is highly sensitive to iron-depleting drugs. The induction of ferroptosis in tumors of the LAR subtype can inhibit tumor growth, improve the immune microenvironment and enhance the efficacy of immune checkpoint blockade therapy (8). In colorectal cancer (CRC), increased expression of microcapsule triglyceride transfer protein in exosomes secreted from the adipose tissues of obese patients can inhibit the occurrence of lipid peroxidation and iron death, thereby reducing chemotherapeutic sensitivity and promoting CRC cell resistance to chemotherapeutics (9). The present study aimed to improve the quality of life of patients and prolong their survival by finding appropriate indicators to

guide clinical medication, reduce overtreatment, improve drug sensitivity and reduce drug resistance.

Materials and methods

Data sources. Data from public databases, including The Cancer Genome Atlas (TCGA; https://portal.gdc.cancer.gov/) and Genotype-Tissue Expression (GTEx; https://gtexportal.org/home/), were used in the present study. TCGA data portal was used to download survival data and tumor staging data for LUAD and LUSC; from a total of 585 cases of LUAD and 504 cases of LUSC. Of these, RNA sequencing data and survival data were available for 516 LUAD cases and 501 LUSC cases. Gene expression profiles were obtained for 59 patients with LUAD and 49 patients with LUSC. Furthermore, data from 578 lung RNA-seq profiles were downloaded from GTEx-lung.

Differential expression analysis of ferroptosis genes. The ferroptosis gene expression profiles of all samples were extracted using R software (version 4.0.3; The R Foundation for Statistical Computing) (10). The ferroptosis genes that were differentially expressed in the tumor group compared with in the non-tumor group were identified using the tidyverse package (www.tidyverse.org) and the Deseq2 package ($P<0.05$) (https://bioconductor.org/packages/release/bioc/html/DESeq2.html). Subsequently, LUAD and LUSC were divided into three groups according to tumor stage and the differential expression of ferroptosis genes between the groups was analyzed. The Wilcoxon rank-sum test was used for statistical analysis of two groups (11), whereas the Kruskal-Wallis test and Dunn's post hoc test was used for multi-group comparisons.

Survival analysis. Survival data were extracted from survminer (https://cran.r-project.org/web/packages/survminer/index.html). Samples were divided into high and low expression groups according to the median value of gene expression. Outcomes included overall survival (OS), disease-free survival (DFS) and progression-free survival (PFS). Kaplan-Meier survival curves (12) were plotted and the log-rank test was performed to analyze the association between the ferroptosis-associated differentially expressed genes and prognostic data. The hazard ratio and 95% CI were used to estimate OS, DFS and PFS.

Association analysis of tumor stage and ferroptosis genes. Sankey diagrams were used to generate graphical representations of the distribution of ferroptosis genes in different tumor stages, and to indicate the relationship between gene expression and patient survival. The R software package ggalluvial was used to construct the Sankey diagram (https://cran.r-project.org/package=ggalluvial). The association between differentially expressed genes and tumor size, lymph node metastasis and distant metastasis was determined using the Kruskal-Wallis test and Dunn's post hoc test.

Immune correlation analysis. The Tumor Immune Estimation Resource (TIMER) score, EPIC score and CIBERSORT were calculated using the R immunedeconv package (v4.0.3) (https://omnideconv.org/immunedeconv/). Tumor immunophenotype (TIP) (https://github.com/dengchunyu/TIP) was calculated using the R immunedeconv package (v4.0.3). The TIMER score is used to estimate the number of immune cells present; EPIC provides the relative proportions of cells; CIBERSORT is used for the assessment of T-cell characteristics; and the proportion of tumor-infiltrating immune cells in the cancer immune cycle can be tracked and analyzed using TIP. The immune correlation network graph was used to visualize the correlation between gene expression and immune scores, and the correlation between immune scores themselves.

Pathway analysis. To clarify the relationship between genes and pathways, the enrichment fraction of each sample in each pathway was calculated using the Single Sample Gene Set Enrichment Analysis (ssGSEA) algorithm (13), and the Spearman correlation between gene expression and the pathway score was calculated.

Immunohistochemical staining. A total of 99 patients with LUAD who had undergone surgery at the Central Hospital Affiliated to Shenyang Medical College (Shenyang, China) and Shengjing Hospital (Shenyang, China) between January 2015 and December 2018 were included in the present study. The patients ranged in age from 36 to 81 years(average age, 58.97±9.49 years), including 55 men and 44 women. Sectioning and immunohistochemical staining were performed using paraffin-embedded tissue sections from patients with a pathological diagnosis of LUAD, which were obtained from the Pathology Department, Central Hospital Affiliated to Shenyang Medical College. The Central Hospital Affiliated to Shenyang Medical College ethics committee reviewed and approved the present study [approval no. Ke-2024-128(02)]. The use of the samples remaining after clinical diagnosis had no adverse effects on the patients; therefore, the need for consent was waived.

For immunohistochemistry, paraffin-embedded sections were collected under Office for Human Research Protections guidelines. Briefly, the paraffin-embedded sections (3 μm), underwent antigen retrieval with citric acid under high pressure for 3 min and were blocked with 3% hydrogen peroxide for 20 min at 24˚C. Subsequently, the sections were incubated with primary antibodies at 4˚C for 12 h and with MaxVision™ HRP-Polymer anti-Mouse/Rabbit secondary antibodies (cat. no. kit5030; Fuzhou Maixin Biotechnology Development Co., Ltd.) at 4˚C for 0.5 h. The sections then underwent DAB staining for 1 min, after which, they were counterstained with hematoxylin for 1 min, sealed with neutral resin and observed under an Olympus BX53 light microscope (Olympus Corporation). The following primary antibodies were used: CDGSH iron-sulfur domain-containing protein 1 (CISD1; 1:100; cat. no. TA500905; Origene Technologies, Inc.), CD4 (1:100; cat. no. RMA-0620; Fuzhou Maixin Biotechnology Development Co., Ltd.) and CD20 (1:100; cat. no. Kit0001; Fuzhou Maixin Biotechnology Development Co., Ltd.)]. Cytoplasmic brown staining was considered positive for immunohistochemistry. The interpretation of the results was the responsibility of two senior pathologists. The degree of CISD1 positivity was categorized as follows: 0, not positive; 1, weakly positive (light yellow); 2, moderately positive (yellowish-brown); and 3, strongly positive (tan). Regarding

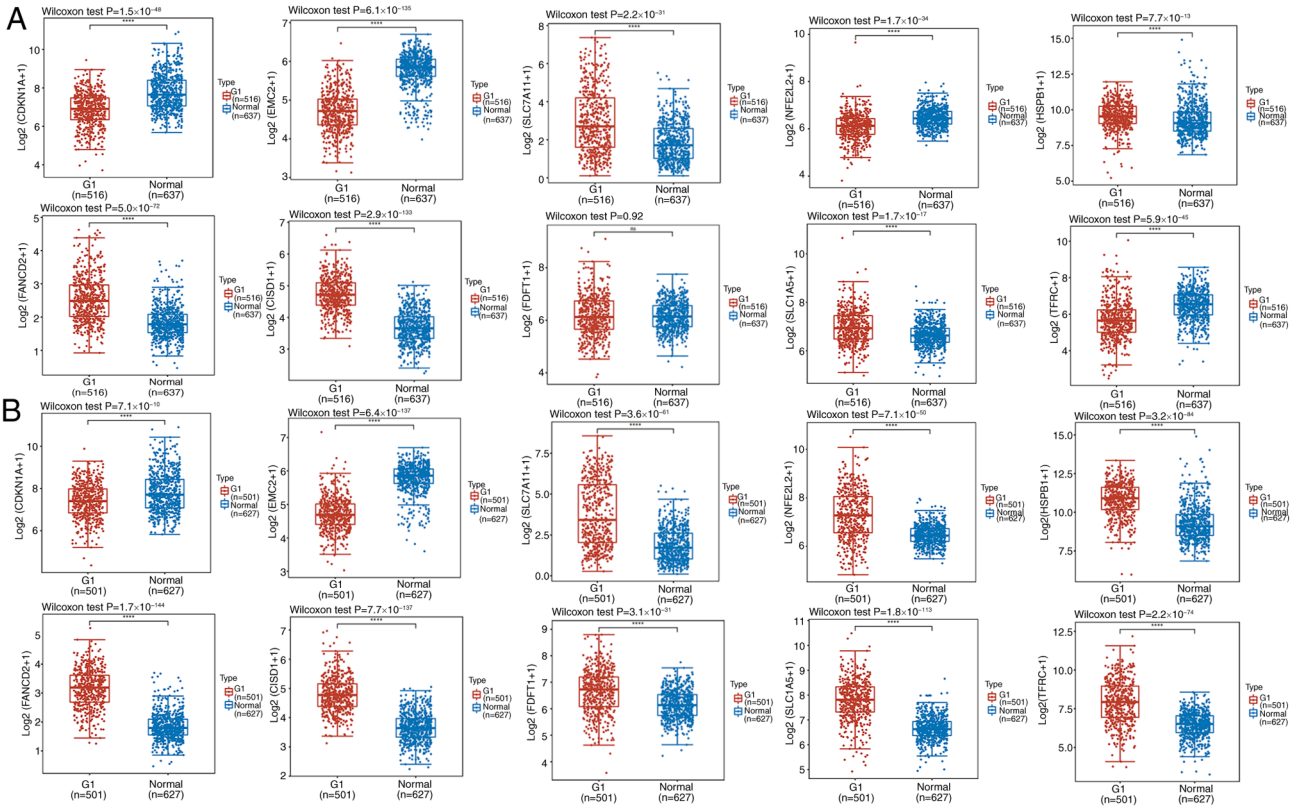

Figure 1. Analysis of differences in ferroptosis gene expression. G1 indicates the tumor group and normal represents the non-tumor group. The non-tumor group comprises paired paracancerous tissues and Genotype-Tissue Expression lung tissues. (A) Box chart of ferroptosis gene expression in the lung adenocarcinoma tumor group and the non-tumor group. (B) Box chart of ferroptosis gene expression in the lung squamous cell carcinoma tumor group and the non-tumor group. The two groups of samples were compared using the Wilcoxon rank-sum test. ****P<0.0001. ns, not significant.

the CISD1 staining area score, a score of 0-100 was assigned according to the percentage of positive tumor cells/total tumor cells. The total staining score was equal to the product of the staining area score and the degree of positivity of the staining results. A total score of ≥100 indicated high CISD1 expression, whereas a total score of <100 indicated low CISD1 expression. For CD4 and CD20 staining, only the percentage of positive cells was calculated.

Statistical analysis. R software (version 4.0.3) was used for both data analysis and visualization. SPSS 17.0 (IBM Corp.) was used for the χ^2 test. Two groups of specimens were compared using the Wilcoxon rank-sum test, whereas three groups of specimens were compared using the Kruskal-Wallis test and Dunn's post hoc test. Spearman correlation analysis was used to analyze the correlation between immunohistochemical scores of clinicopathological indicators, and Kaplan-Meier analysis and log-rank test was used for survival analysis (SPSS v17.0). P<0.05 was considered to indicate a statistically significant difference.

Results

Differential expression of iron-depleting genes in tumor and non-tumor tissues. Data for 516 cases of LUAD and 59 matched samples of paracancerous tissues, and 501 cases of LUSC and 49 matched samples of paracancerous tissues were downloaded from TCGA. A total of 578 lung tissue samples without disease in GTEx were included due to the small amount of data in the control group. Differences between the tumor and non-tumor groups were analyzed by extracting the expression profiles of >20 classical ferroptosis genes. Compared with those in normal tissues, the expression levels of SLC7A1, HSPB1, FANCD2, CISD1, HSPA5, NCOA4, GPX4, DPP4, RPL8 and SLC1A5 were upregulated in LUAD cancer tissues, whereas the expression levels of CDKN1A, EMC2, NFE2L2, MT1G, LPCAT3, GLS2, SAT1, CS, ALOX1, ACSL4, ATL1 and TFRC were downregulated (Figs. 1A and S1A). In LUSC cancer tissues, the expression levels of SLC7A1, NFE2L2, HSPB1, FANCD2, CISD1, FDFT1, SLC1A5, HSPA5, NCOA4, GPX4, RPL8 and TFRC were upregulated, whereas the expression levels of CDKN1A,LPCAT3, GLS2, SAT1, DPP4, CS, ACSL4, ATL1 and EMC2 were downregulated (Figs. 1B and S1B).

Differential expression of ferroptosis genes based on tumor clinical stages. Patients with LUAD and LUSC were grouped based on Tumor-Node-Metastasis (TNM) stage. Patients with LUAD or LUSC were divided into three groups, G1 corresponds to stage I, G2 corresponds to stage II, G3 corresponds to stage III and G4 corresponds to stage IV. MT1G, CISD1, RPL8, GLS2, CS, CARS1, ATP5M3 and ACSL4 were associated with the TNM stage of LUAD (Fig. 2A and B). CDKN1A, EMC2 CISD1, TFRC, ALOX15 and ATL1 were associated with the TNM stage of LUSC (Fig. 2C and D). CISD1 was identified in both LUAD and LUSC.

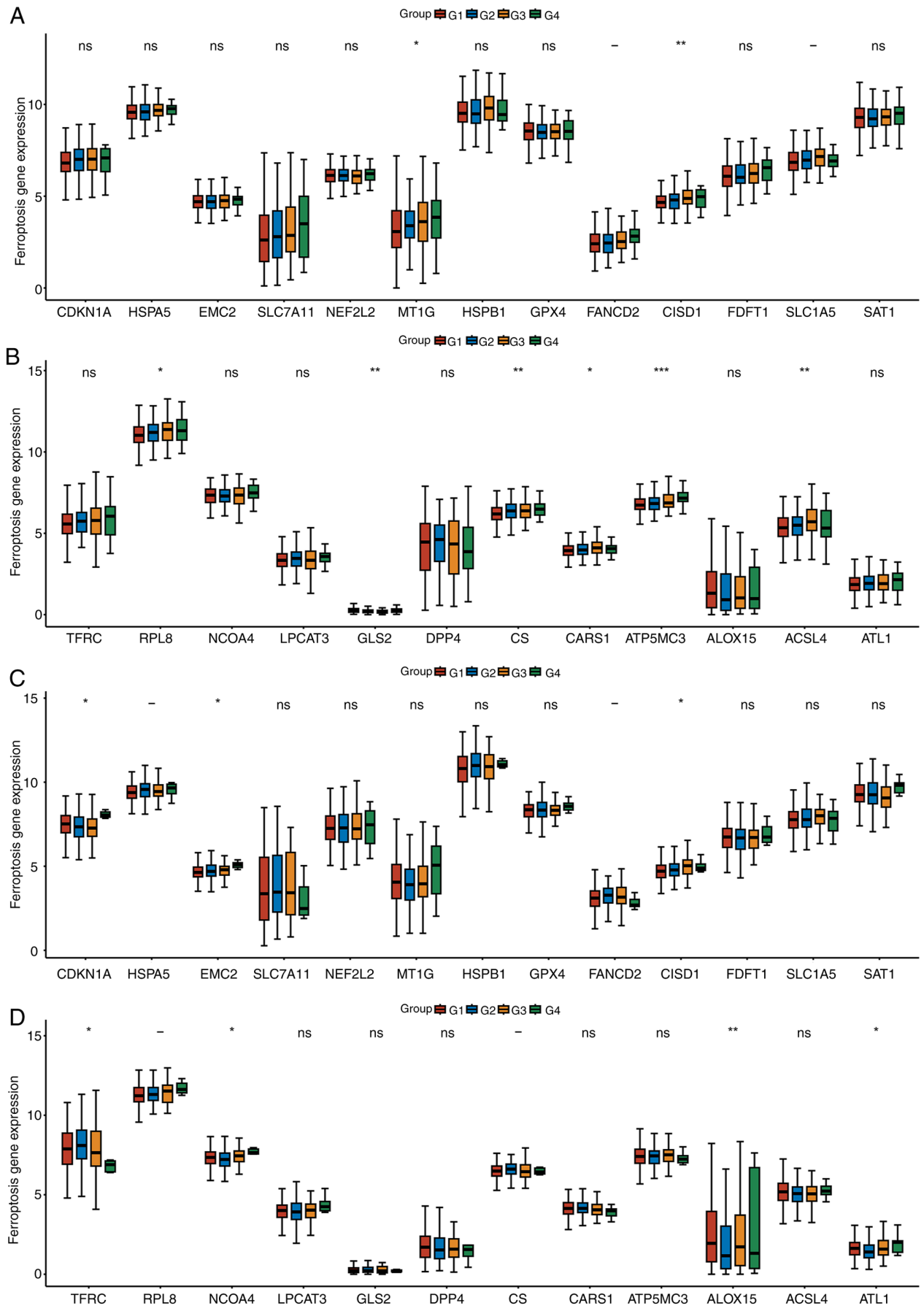

Figure 2. Differential analysis of ferroptosis genes in various clinical tumor stages. (A and B) Differential analysis of ferroptosis genes in lung adenocarcinoma. (C and D) Differential analysis of ferroptosis genes in lung squamous cell carcinoma. G1 corresponds to stage I, G2 corresponds to stage II, G3 corresponds to stage III and G4 corresponds to stage IV. The three groups of samples were compared using the Kruskal-Wallis test. *P<0.05, **P<0.01, ***P<0.001. ns, not significant.

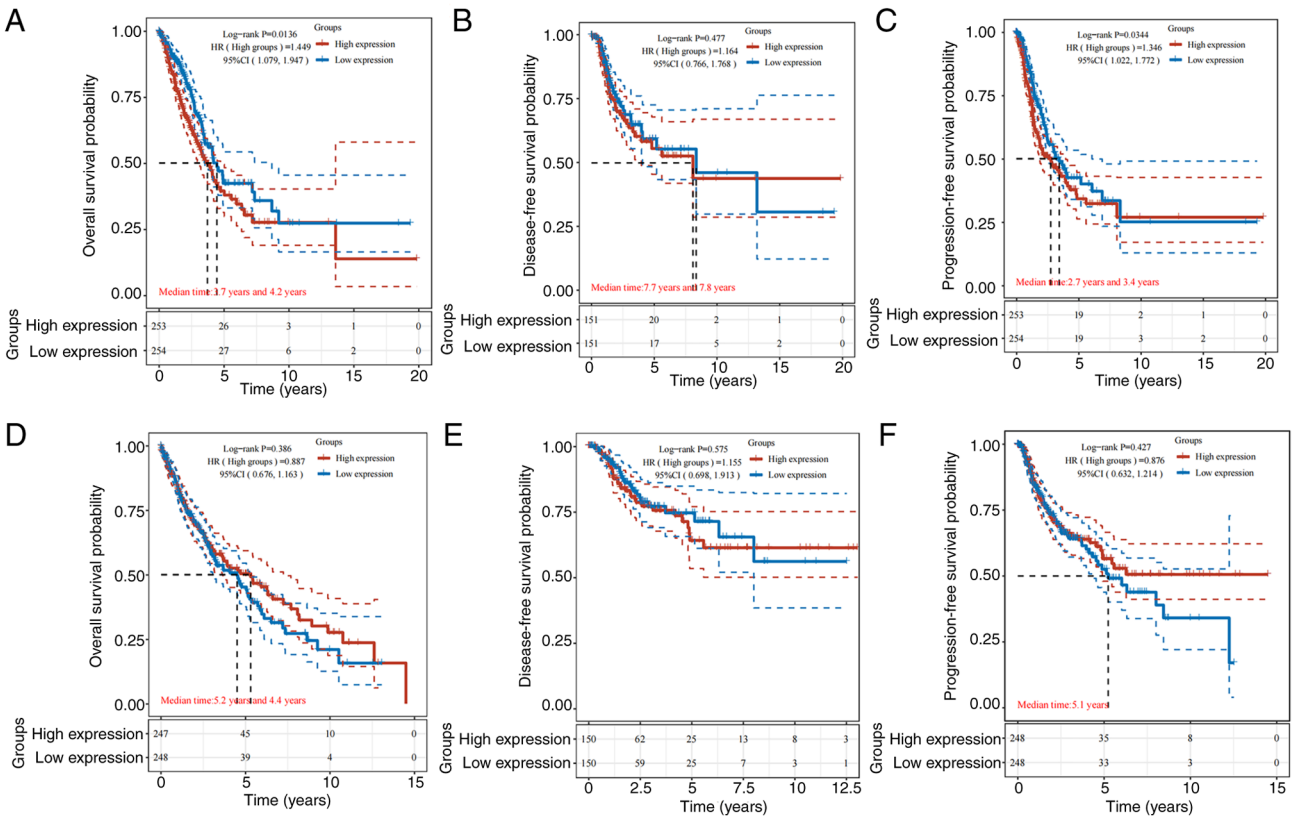

Figure 3. Association of CISD1 with the prognosis of LUAD and LUSC. (A) CISD1 was associated with OS in LUAD; high CISD1 expression was associated with low OS. (B) CISD1 was not associated with DFS in LUAD. (C) CISD1 was associated with PFS in LUAD; high CISD1 expression was associated with poor prognosis. CISD1 was not associated with (D) OS, (E) DFS or (F) PFS in LUSC. CISD1, CDGSH iron-sulfur domain-containing protein 1; DFS, disease-free survival; OS, overall survival; PFS, progression-free survival.

Association between differentially expressed genes and prognosis. LUAD and LUSC differ in how they are treated and prognosticated. For the prognosis of LUAD and LUSC, CISD1 was further analyzed. The results revealed that in LUAD, CISD1 was associated with prognosis, and high levels were associated with lower OS and PFS ($P<0.05$; Fig. 3A and C). This suggested that high levels of CISD1 were associated with poor prognosis. In LUSC, CISD1 was not associated with prognosis (Fig. 3D-F). The relationship between CISD1 and LUAD was thus focused on.

Analysis of the association between CISD1 and clinical characteristics. There were 187 deaths and 329 survivors among all patients with lung cancer from TCGA. Among the patients who died, there were 69 cases in stage I, 55 cases in stage II, 47 cases in stage III and 16 cases in stage IV, including 111 cases (58.73%) with high CISD1 expression and 76 cases (40.64%) with low CISD1 expression. Among the surviving patients, 147 patients (44.68%) were in the high-level CISD1 group and 182 patients (55.32%) were in the low-level CISD1 group. Although 58.73% of the dead patients had high expression of CISD1, it was mainly concentrated in stage I and II, suggesting that the high expression may delay rather than completely prevent the disease progression. By contrast, patients with low expression were more distributed in stages III and IV, and were associated with 62.5% of stage IV deaths, highlighting its strong association with aggressive phenotypes. Patients with low expression of CISD1 accounted for 55.32% of the survival cohort, which may reflect the effectiveness of early intervention for patients with low expression, or the existence of other compensatory pathways to maintain survival (Fig. 4A). Patients with high expression of CISD1 accounted for 42.0% of patients with T1 cancer, and the survival rate (67.6%) was lower in the high-expression group than that in the low-expression group (79.6%). Notably, the survival rate of patients with high CISD1 expression in T4 stage was low (16.7%), which was in sharp contrast with the low-expression group (71.4%) (Fig. 4B). The survival rate of patients with low CISD1 expression in N0 stage was 76.4% (139/182), which was significantly higher than that of patients with high expression (69.3%), suggesting that CISD1 inhibition may improve the prognosis through immune regulation in the metastasis-free stage. However, the survival rate of patients with high expression in N1-N2 stage decreased sharply (N1: 42.4%; N2: 36.4%), and was significantly lower than that of patients with low expression in the same period, suggesting that CISD1 may drive malignant progression by enhancing tumor cell adaptability (such as antioxidant defense) in lymph node metastasis (Fig. 4C). In M0 stage, high CISD1 expression accounted for 52.4%, and its survival rate (56.6%) was lower than that of the low expression group (67.3%). In M1 stage, high CISD1 expression accounted for 64.0%, and its survival rate (31.3%) was lower than that in the low expression group (55.6%) (Fig. 4D). High CISD1 expression may exacerbate adverse outcomes by promoting metastasis or treatment resistance. However, the χ^2 test showed that the level of CISD1 was associated with the

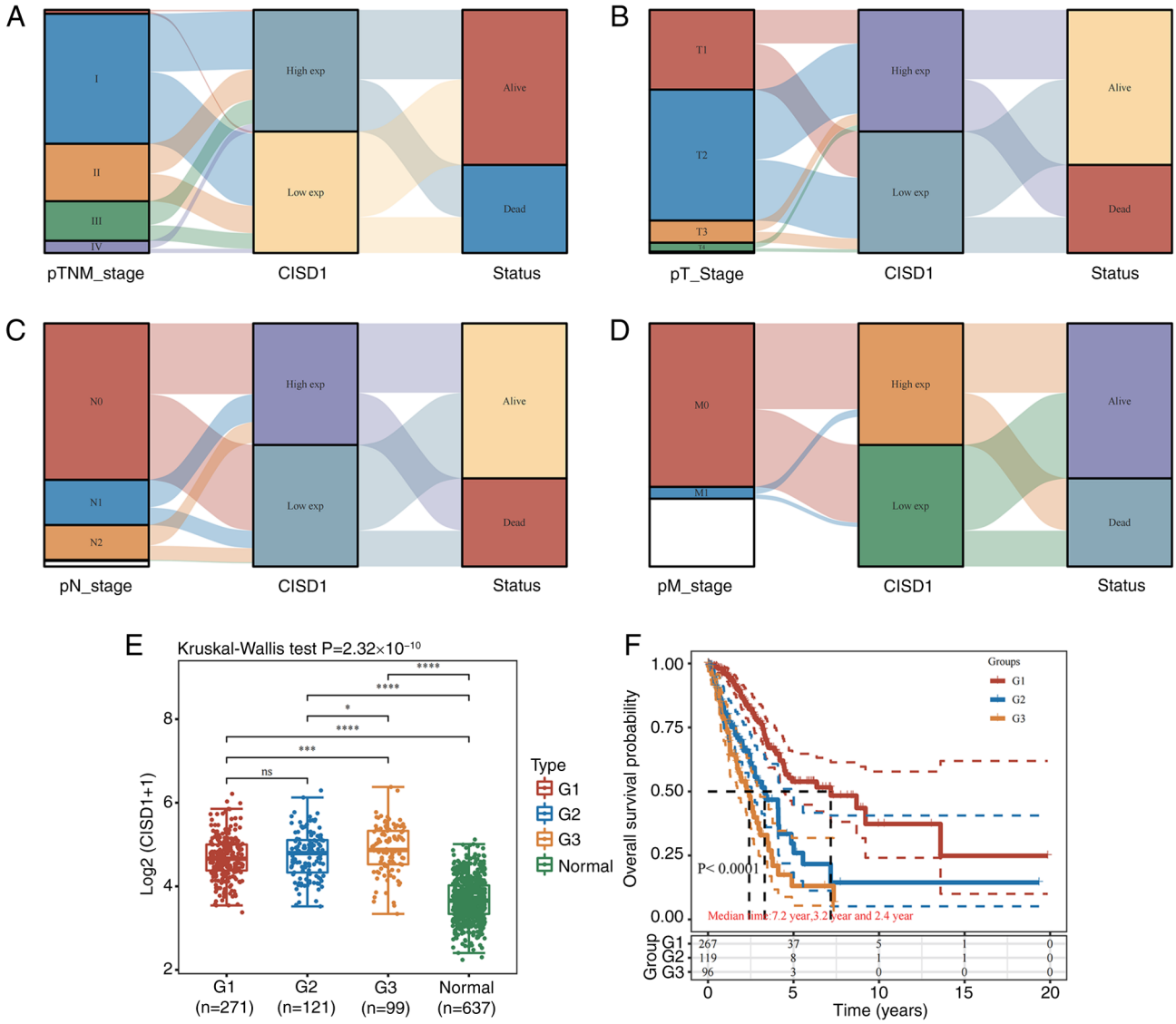

Figure 4. Association between CISD1 and the clinical features in lung adenocarcinoma. (A) Distribution trend of CISD1 and patient outcomes for different clinical stages. (B) Distribution trend of CISD1 and patient outcomes for different tumor sizes. (C) Distribution trend of CISD1 and patient outcomes for lymph node metastasis. (D) Distribution trend of CISD1 and patient outcomes for distant metastasis. (E) Association between CISD1 expression and different clinical stages. *P<0.05, ***P<0.001,****P<0.0001. (F) Relationship between different tumor stages and the prognosis of lung adenocarcinoma. CISD1, CDGSH iron-sulfur domain-containing protein 1; M0, no distant metastasis; M1, distant metastasis; N0, no lymph node metastasis; N1, ipsilateral pulmonary lymph node metastasis; N2, lymph node metastasis within the mediastinum or below the protuberance on the same side; T1, ≤3 cm; T2, >3-5 cm; T3, >5-7 cm; T4, >7 cm; ns, not significant.

outcome; a high level of CISD1 could indicate a poor outcome (Table I). In order to exclude intra-group differences, different clinical stages and non-tumor tissues were also compared. CISD1 expression was positively associated with TNM stage (Fig. 4E), and TNM stage was closely associated with tumor prognosis (Fig. 4F). This suggested that, when CISD1 expression was high in patients, the risk of adverse outcomes was also high. It is recommended that consideration be given to the addition of ferroptosis-related drugs in the design of treatment plans for patients.

Association between CISD1 and immunity. The present study further analyzed the association between CISD1 and immunity to explore the potential application value of targeting ferroptosis in the immunotherapy of LUAD. The network connection diagram and heat map were used to visualize the association between gene expression and the immune score (Fig. 5). The more red or blue, the stronger the correlation between both, and the larger the ring, the stronger the correlation. The red line represents a positive correlation between the model score or the gene expression and the immune score, and the green line represents a negative correlation between the two. The TIMER score (Fig. 5A), EPIC score (Fig. 5B), CIBERSORT score (Fig. 5C) and TIP score (Fig. 5D) showed that CISD1 was negatively correlated with $CD4^+$ T cells and B cells.

CISD1 and pathways. The ssGSEA algorithm was used to calculate the enrichment fraction of each sample for a given pathway to investigate the relationship between samples and pathways. These calculated enrichment fractions provided an intuitive way to show how samples and pathways interacted and were associated. The results suggested that CISD1

Table I. χ^2 test of the relationship between CISD1 expression level and clinical outcome.

Characteristic	CISD1 expression		Pearson χ^2 value	P-value
	High	Low		
Clinical outcome				
Alive	147	182	10.274	0.001
Dead	111	76		

CISD1, CDGSH iron-sulfur domain-containing protein 1.

may be involved in the cellular response to hypoxia, DNA repair, extracellular matrix-related genes, epithelial-mesenchymal transition markers, oxidative phosphorylation, PI3K-AKT-mTOR signaling pathway and metabolic pathways (glycine, serine and threonine metabolism; D arginine and D ornithine metabolism; alanine, aspartate and glutamate metabolism; biotin metabolism) in LUAD (Fig. 6).

CISD1 expression in cancer tissues and prognosis. CISD1 expression in LUAD cancer tissues (Fig. 7A and B) was significantly higher than that in adjacent tissues (Fig. 7C and D), as determined using Wilcoxon rank-sum test (P<0.001; Z=-7.471; Fig. 7E). In LUAD, the χ^2 test indicated that CISD1 was positively associated with lymph node metastasis (P=0.010; χ^2=6.559), and Ki67 (P=0.005; χ^2=7.932) (Table II). By contrast, CISD1 was not associated with sex, tumor differentiation, tumor size and TNM in patients with LUAD. Furthermore, high CISD1 expression indicated poor prognosis and a shorter DFS (P=0.002; Fig. 7F).

A total of 60 cases were randomly selected for CD4 and CD20 staining. The results demonstrated that the expression levels of CISD1 in LUAD were negatively associated with the infiltration of immune cells. The number of CD4 cells was lower in cases with high CISD1 expression (Fig. 8A and B), and the number of CD20 cells was also lower (Fig. 8F and G). The number of CD4 and CD20 immune cells was higher in cases with low CISD1 expression (Fig. 8D, E, I and J). CISD1 was negatively associated with the immune infiltration of CD4 (P<0.001; Z=-6.575) and CD20 (P<0.001; Z=-5.970) cells using Wilcoxon signed-rank test (Fig. 8C and H).

Discussion

Early detection and treatment are important tools for the improvement of the survival rate of patients with lung cancer. The advent of personalized and targeted therapies has served a positive role in prolonging patient survival, improving the treatment response and quality of life of patients. However, the correct application of these novel regimens and methods is highly dependent on appropriate molecular typing. For NSCLC, detecting EGFR, ALK and ROS1 gene mutations can guide targeted medication (14). The in-depth analysis of the molecular characteristics of lung cancer genes and proteins can provide an important basis for the development of targeted treatments.

The incidence of LUAD is generally higher than that of LUSC (15,16). CISD1 is a potential gene that is related to the stage of the tumor; however, the present study revealed that CISD1 was not associated with prognosis in LUSC. Therefore, the study focused on the role of CISD1 in LUAD. CISD1 is known to belong to the mitoNEET family, other members of which include CISD2 and CISD3 (17,18). The CISD1 gene is located at chromosome 10q21.1 and the encoded protein is located in the outer membrane of mitochondria. CISD1 is an L-cysteine aminotransferase that catalyzes the reversible transfer of amino groups from L-cysteine to α-keto acids and 2-oxoglutarate to form 2-oxo-3-thiopropionate and L-glutamic acid, respectively (19). CISD1 was originally considered to be targeted by pioglitazone, a drug used to treat diabetes (20). A previous study demonstrated that in breast cancer, CISD1 expression is higher in tumor tissues than in normal tissues, and that it is positively associated with poor OS (21). Liang *et al* (22) constructed a prognostic model including CISD1 for bladder cancer and proposed that this model was independently associated with OS. This is consistent with the present findings. The present results demonstrated that CISD1 was positively associated with poor OS and PFS in LUAD. However, Yang *et al* (23) constructed pancreatic adenocarcinoma prognosis models including CISD1 and proposed that CISD1 was a tumor suppressor gene, thus suggesting that CISD1 may serve different roles in different tumors.

CISD1 is closely related to the immune microenvironment. Notably, there is a negative association between CISD1 and regulatory T cells or plasma cells in patients with asthma, and CISD1 has been reported to be upregulated in mild to moderate asthma and severe asthma (24). Furthermore, the changes of the immune microenvironment in psoriasis may be related to PRKAA2, PEBP1, CISD1 and acsf2 (25). A previous study reported that cigarette smoke can induce the reduction of CISD1 in macrophages, and promotes M1 polarization and mitochondrial dysfunction by activating the autophagy pathway, thus promoting the occurrence and development of chronic obstructive pulmonary disease (26). In addition, ferroptosis is associated with immune processes such as T-cell function, immune checkpoints, human leukocyte antigen and T-cell co-stimulation (27). CISD1 has been shown to be associated with the prognosis of patients with hepatocellular carcinoma, and the immune infiltration levels of $CD8^+$ T cells, macrophages, neutrophils and dendritic cells (28). Higher CISD1 expression in gastric cancer tissues is also related to an increase in tumor size, differentiation, depth of invasion and lymph node metastasis. Furthermore, CISD1 upregulation indicates poor OS of patients with gastric cancer, and it is expected to participate in the regulation of gastric cancer immune cell infiltration as an ferroptosis inhibitor (29). In the present study, immunohistochemical staining indicated that CISD1 was associated with immune infiltration, and CISD1 was negatively associated with $CD4^+$ T cells and $CD20^+$ B cells.

Ferroptosis and immunity have potential applications (30). In the process of ferroptosis, ferrous sulfate can be used as a source of iron for participation in the Fenton reaction and production of excessive ROS, thus inducing ferroptosis (31). Ferrous sulfate can interfere with normal iron metabolism by combining with iron; this leads to iron

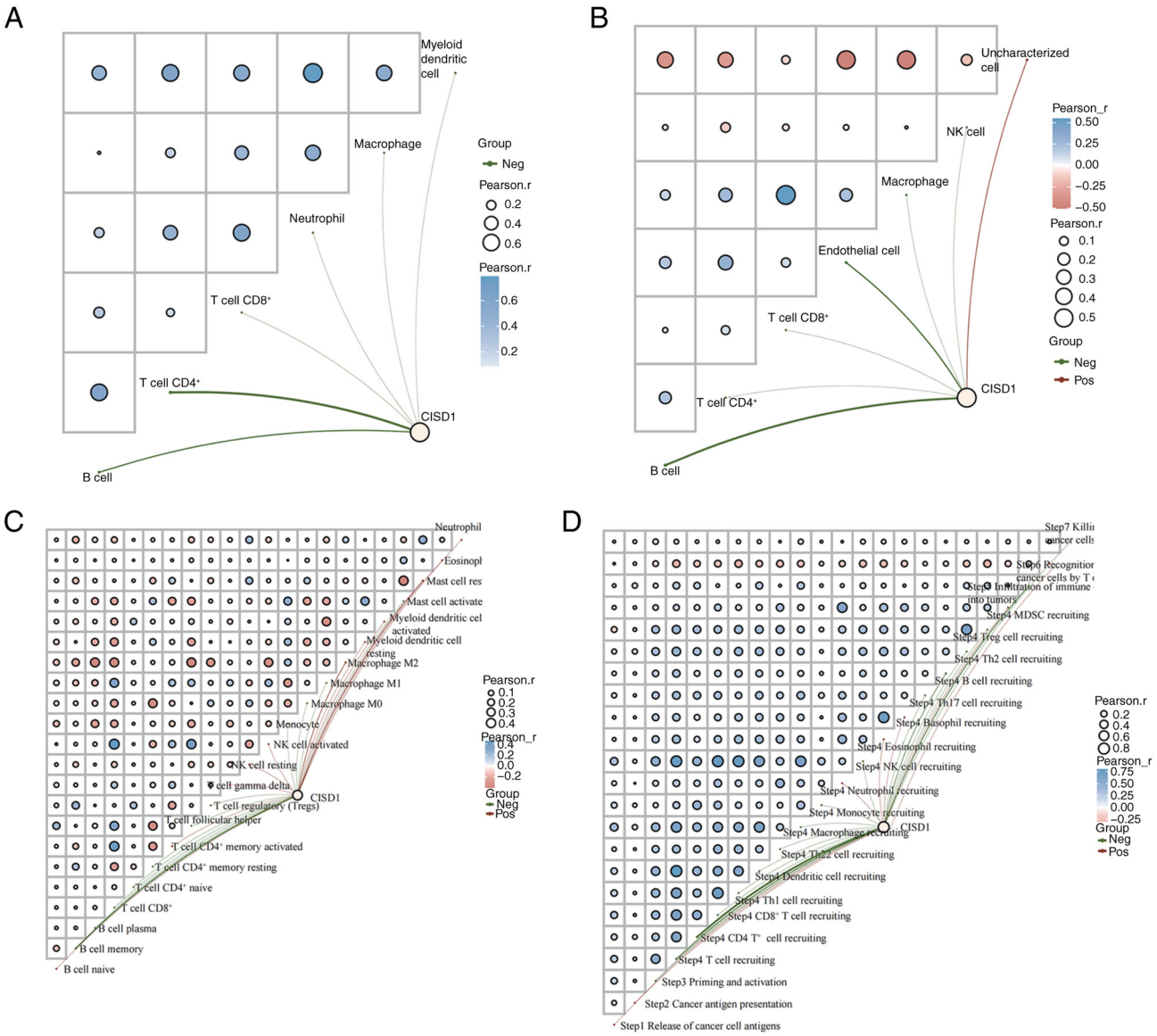

Figure 5. Immune correlation analysis. (A) The Tumor Immune Estimation Resource score was used to estimate the number of immune cells. (B) EPIC score indicating the relative composition of cells. (C) The CIBERSORT score was used to evaluate the characteristics of T cells. (D) The tumor immunophenotype score was used to track and analyze the proportion of tumor-infiltrating immune cells in the cancer immune cycle. Red indicates a positive correlation and blue indicates a negative correlation

accumulation in cells, which then causes lipid peroxidation and cell death (32). CISD1 is closely related to the aging of organisms and mitochondria. A previous study reported that CISD1 regulates the longevity of *Caenorhabditis elegans* by participating in autophagy and mitochondrial internal apoptosis pathways, and regulates protein homeostasis and aging (33). Furthermore, CISD1 deficiency can lead to iron transport imbalance and proton leakage, and can reduce ATP production by interrupting the mitochondrial electron transport chain (34). CISD1 expression has been reported to be specifically downregulated in the heart and kidney of aging mice, which may cause the heart mitochondria to gradually lose their integrity in the process of natural aging (35). Furthermore, CISD1 accumulates in *Drosophila melanogaster* during the aging process. By contrast, reducing the levels of CISD1 can improve the pathological phenotype of the movement, life span and neurodegeneration of *D. melanogaster*; therefore, inhibition of CISD1 may provide a potential target for therapeutic intervention (36).

Based on the research of aging-related diseases, PTEN induced kinase 1 and parkin regulate estrogen receptor calcium release through CISD1 and inositol 1,4,5-trisphosphate receptor, and are feasible targets for the treatment of Parkinson's disease (37). Additionally, in the field of neurological research, targeting CISD1 signaling is considered to be a novel therapeutic strategy for the prevention and treatment of neonatal hypoxic-ischemic injury caused by perinatal asphyxia (38). Furthermore, CISD1 is a mediator of ferroptosis in neural stem cells, and its expression is enhanced due to high fructose levels, driving the death of hippocampal neural stem cells, resulting in a decreased sweet taste preference (39). Gastrodin can alleviate CISD1-mediated ferroptosis (39). In a lung injury-related study, CISD1 inhibition by mitoNEET ligand-1 was shown to reduce lipopolysaccharide-induced

Table II. χ^2 test of the relationship between CISD1 expression and clinicopathological parameters.

Characteristic	n	CISD1 High expression (n=57)	CISD1 Low expression (n=42)	Pearson χ^2 value	P-value
Sex					
Male	44	26	18	0.074	0.785
Female	55	31	24		
Tumor differentiation					
Well	36	19	17	1.053	0.591
Moderate	52	24	18		
Poor	21	14	7		
Tumor size					
≤3.0 cm	59	32	27	1.819	0.403
>3 cm and ≤5 cm	25	14	11		
>5 cm	15	11	4		
Lymph node metastasis					
Positive	43	31	12	6.559	0.010
Negative	56	26	30		
TNM					
I	43	19	24	5.887	0.053
II	46	32	14		
III	10	6	4		
Ki-67					
>10%	70	34	36	7.932	0.005
≤10%	29	23	6		

CISD1, CDGSH iron-sulfur domain-containing protein 1; TNM, Tumor-Node-Metastasis.

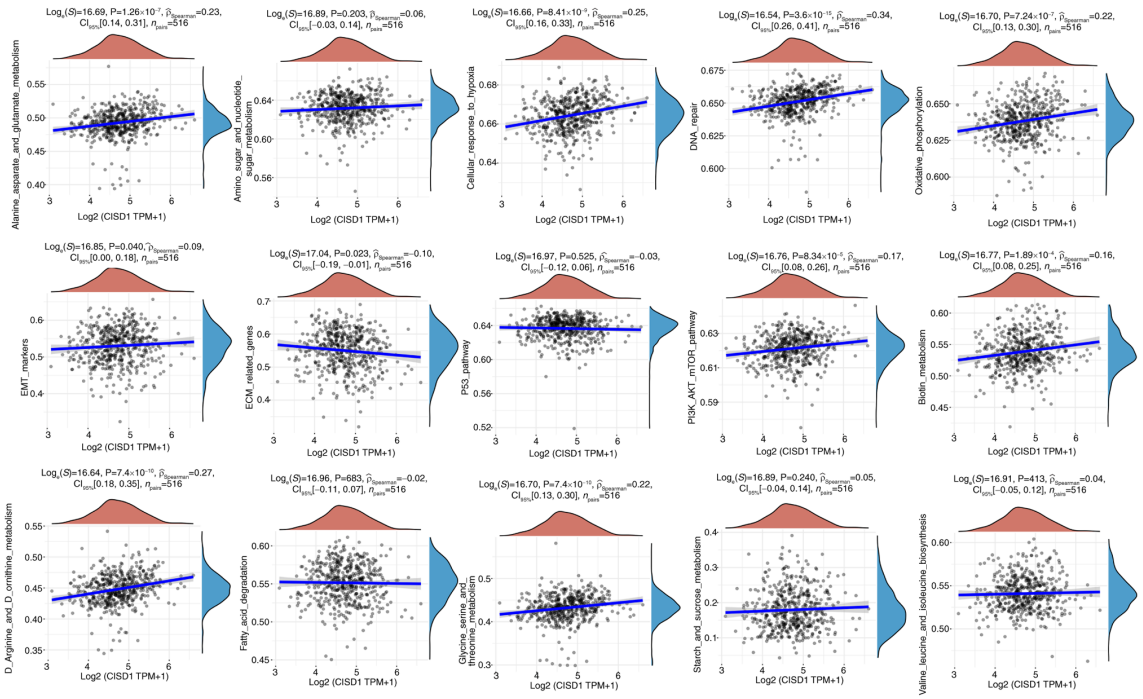

Figure 6. ssGSEA of the correlation of CISD1 and signaling pathways in LUAD. By applying the ssGSEA algorithm, detailed calculations were conducted on the enrichment scores of each sample on specific pathways to explore the relationship between samples and pathways. CISD1 may be involved in DNA repair, extracellular matrix-related genes, epithelial-mesenchymal transition markers, oxidative phosphorylation, PI3K-AKT-mTOR signaling pathway and other metabolic pathways in LUAD. CISD1, CDGSH iron-sulfur domain-containing protein 1; LUAD, lung adenocarcinoma; ssGSEA, Single Sample Gene Set Enrichment Analysis.

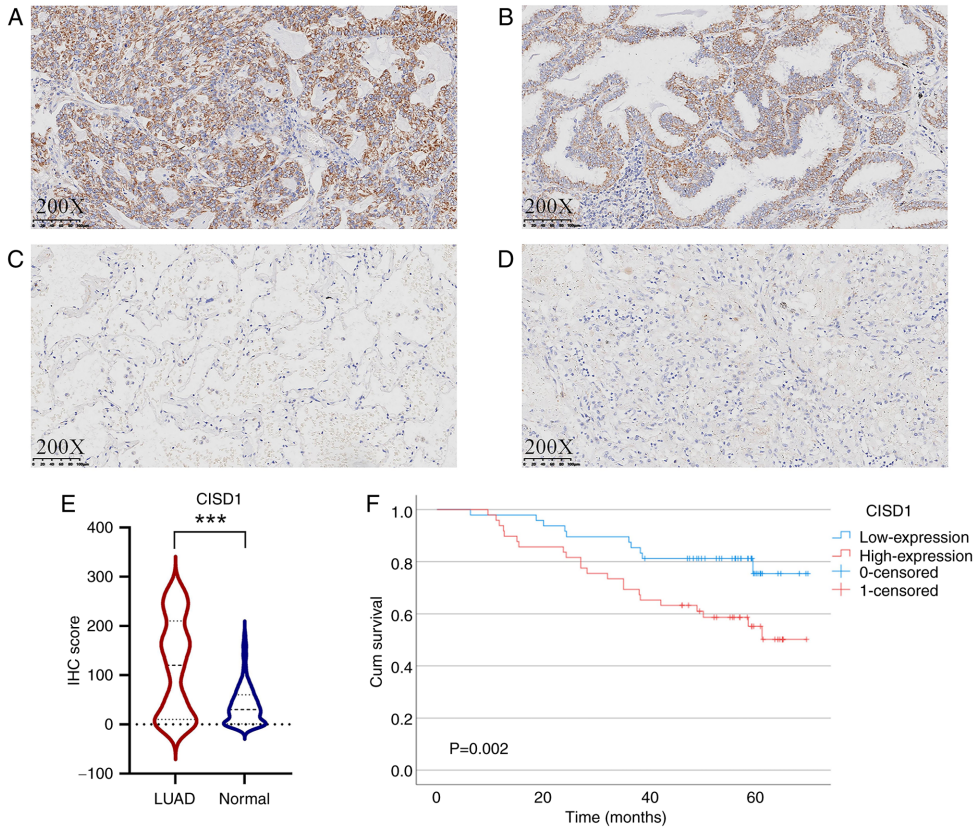

Figure 7. CISD1 protein expression in LUAD. (A) IHC staining for CISD1 was positive in one patient with LUAD. (B) IHC staining for CISD1 was positive in another patient with LUAD. (C) IHC staining for CISD1 was negative in paracancerous tissue; this tissue was from the patient in (A). (D) IHC staining for CISD1 was negative in paracancerous tissue; this tissue was from the patient in (B). (E) Comparison of CISD1 expression between cancerous tissues and adjacent non-cancerous tissues in LUAD. (F) Association between CISD1 expression in LUAD and patient prognosis. ***P<0.001. CISD1, CDGSH iron-sulfur domain-containing protein 1; IHC, immunohistochemistry; LUAD, lung adenocarcinoma.

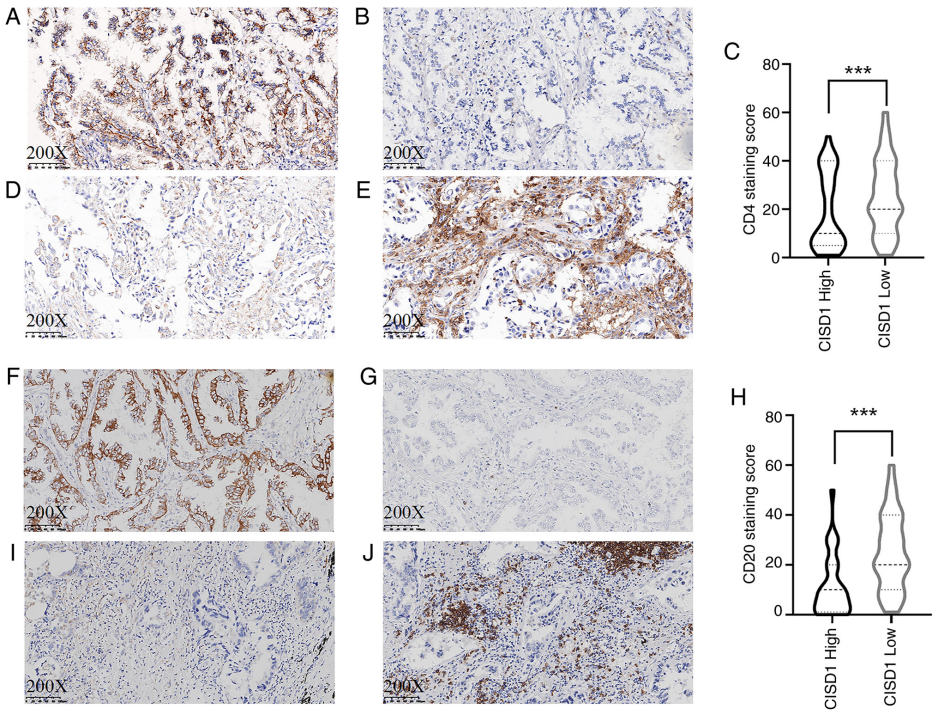

Figure 8. Association between CISD1 expression and CD4 and CD20 in LUAD tissues. (A) High expression of CISD1 and (B) low expression of CD4 in one patient with LUAD. (C) Violin plot of CISD1 and CD4 protein expression levels in LUAD. (D) Low CISD1 expression and (E) high CD4 expression in one patient with LUAD. (F) High expression of CISD1 and (G) low CD20 expression in one patient with LUAD. (H) Violin plot of CISD1 and CD20 protein expression levels in LUAD. (I) Low CISD1 expression and (J) high CD4 expression in one patient with LUAD. ***P<0.001. CISD1, CDGSH iron-sulfur domain-containing protein 1; LUAD, lung adenocarcinoma.

iron death *in vivo* and *in vitro*, reduce pathological injury and pulmonary edema, and reduce the levels of IL-6, IL-1β and TNF-α in the lungs and bronchoalveolar lavage fluid of mice with acute lung injury (40).

The GCN5L1/CSID1 axis is crucial for oxidative stress and ethanol-induced ferroptosis (41). Early iron-dependent cell death releases a number of damage-related molecular patterns, which can effectively activate bone marrow-derived dendritic cells by inhibiting glutathione peroxidase 4-induced cancer cell ferroptosis, and subsequently induce antitumor adaptive immunity, which can activate the immune system, aiding the treatment of tumors (42). In a tumor-related study, targeted inhibition of CISD1 has been shown to reduce ROS accumulation, mitochondrial dysfunction and apoptosis through PI3K and MAPK pathways (43). CISD1 knockout also leads to changes in mitochondrial ultrastructure and function, increased ROS and decreased cell proliferation. In addition, CISD1 may be used as a drug target for the treatment of minimal residual leukemia (44). In the present study, increased CISD1 was detected in LUAD tissues, and was associated with worse staging and prognosis; therefore, CISD1 may be an effect target for the treatment of LUAD.

In conclusion, the prognosis of LUAD was associated with CISD1, a ferroptosis gene. Through the regulation of CISD1, it may be possible to influence the immune microenvironment of LUAD to a certain extent. The development of safe and effective targeted drugs against CISD1 is a direction worthy of future consideration and exploration.

Acknowledgements

Not applicable.

Funding

The present study was supported by the 2022 Shenyang Science and Technology Plan (grant no. 22-321-33-94) and the 2023 Liaoning Provincial Department of Education (grant no. JYTMS20231387).

Availability of data and materials

The data generated in the present study may be requested from the corresponding author

Authors' contributions

XL designed the present study. TW conducted the experiments and wrote the manuscript. XL, XX, ZZ and TW performed the experiments, collected data and confirm the authenticity of all the raw data. All authors read and approved the final version of the manuscript.

Ethics approval and consent to participate

The present study was approved by the Ethics Committee of the Central Hospital Affiliated to Shenyang Medical College [approval no. Ke-2024-128(02)]. A waiver of informed consent was granted under 45 CFR 46.104 due to the use of de-identified retrospective data.

Patient consent for publication

Not applicable.

Competing interests

The authors declare that they have no competing interests.

References

1. Han B, Zheng R, Zeng H, Wang S, Sun K, Chen R, Li L, Wei W and He J: Cancer incidence and mortality in China, 2022. J Natl Cancer Cent 4: 47-53, 2024.
2. Li C, Lei S, Ding L, Xu Y, Wu X, Wang H, Zhang Z, Gao T, Zhang Y and Li L: Global burden and trends of lung cancer incidence and mortality. Chin Med J (Engl) 136: 1583-1590, 2023.
3. Ettinger DS, Wood DE, Aisner DL, Akerley W, Bauman J, Chirieac LR, D'Amico TA, DeCamp MM, Dilling TJ, Dobelbower M, *et al*: Non-small cell lung cancer, version 5.2017, NCCN clinical practice guidelines in oncology. J Natl Compr Canc Netw 15: 504-535, 2017.
4. Lim ZF and Ma PC: Emerging insights of tumor heterogeneity and drug resistance mechanisms in lung cancer targeted therapy. J Hematol Oncol 12: 134, 2019.
5. Dixon SJ, Lemberg KM, Lamprecht MR, Skouta R, Zaitsev EM, Gleason CE, Patel DN, Bauer AJ, Cantley AM, Yang WS, *et al*: Iron death: An iron dependent form of nonapoptotic cell death. Cell 149: 1060-1072, 2012.
6. Park E and Chung SW: Ros-mediated autophagy increases intracellular iron levels and ferropositis by ferritin and transferrin receptor regulation. Cell death Dis 10: 822, 2019.
7. Conche C, Finkelmeier F, PEšIć M, Nicolas AM, Böttger TW, Kennel KB, Denk D, Ceteci F, Mohs K, Engel E, *et al*: Combining osteoporosis induction with MDSC blockade renders primary tumours and metals in liver sensitive to immune checkpoint blockade. Gut 7: 1774-1782, 2023.
8. Yang F, Xiao Y, Ding JH, Jin X, Ma D, Li DQ, Shi JX, Huang W, Wang YP, Jiang YZ and Shao ZM: Ferroptosis heterogeneity in triple-negative breast cancer reveals an innovative immunotherapy combination strategy. Cell Metab 35: 84-100.e8, 2023.
9. Zhang Q, Deng T, Zhang H, Zuo D, Zhu Q, Bai M, Liu R, Ning T, Zhang L, Yu Z, *et al*: Adipocyte-derived exosomal MTTP suppresses ferrooposis and promotes chemoresistance in colorectal cancer. Adv SCI (Weinh) 9: e2203357, 2022.
10. Wang J, Wang L, Pang Z, Ge Q, Wu Y and Qi X: Integrated analysis of ferroptosis and immunity-related genes associated with diabetic kidney disease. Diabetes Metab Syndr Obes 16: 3773-3793, 2023.
11. Hsieh SS, Cook DA, Inoue A, Gong H, Sudhir Pillai P, Johnson MP, Leng S, Yu L, Fidler JL, Holmes DR III, *et al*: Understanding reader variability: A 25-radiologist study on liver metastasis detection at CT. Radiology 306: e220266, 2023.
12. Messori A: Synthetizing published evidence on survival by reconstruction of patient-level data and generation of a multi-trial kaplan-meier curve. Cureus 13: e19422, 2021.
13. Cao L, Liu M, Ma X, Rong P, Zhang J and Wang W: Comprehensive scRNA-seq analysis and identification of CD8_+T cell related gene markers for predicting prognosis and drug resistance of hepatocellular carcinoma. Curr Med Chem 31: 2414-2430, 2024.
14. Kalemkerian GP, Narula N, Kennedy EB, Biermann WA, Donington J, Leighl NB, Lew M, Pantelas J, Ramalingam SS, Reck M, *et al*: Molecular testing guideline for the selection of lung cancer patients for treatment with targeted thyroid kinase inhibitors: American society of clinical oncology endowment summary of the college of American physicians/international association for the study of lung cancer/association for molecular pathology clinical practice guideline update. J Clin Oncol 36: 911-919, 2018.
15. Fukui T, Taniguchi T, Kawaguchi K, Fukumoto K, Nakamura S, Sakao Y and Yokoi K: Comparisons of the clinicopathological features and survival outcomes between lung cancer patients with adenocarcinoma and rectangular cell carcinoma. Gen Thorac Cardiovasc Surg 63: 507-513, 2015.
16. Wang BY, Huang JY, Chen HC, Lin CH, Lin SH, Hung WH and Cheng YF: The comparison between adenocarcinoma and rectangular cell carcinoma in lung cancer patients. J Cancer Res Clin Oncol 146: 43-52, 2020.

17. Wiley SE, Murphy AN, Ross SA, van der Geer P and Dixon JE: Mitoneet is an iron containing outer mitochondrial membrane protein that regulates oxidative capacity. Proc Natl Acad SCI USA 104: 5318-5323, 2007.
18. Inupakutika MA, Sengupta S, Nechushtai R, Jennings PA, Onuchic JN, Azad RK, Padilla P and Mittler R: Phylogenetic analysis of eucaryotic neet proteins uncovers a link between a key gene duplication event and the evolution of vertebrates. Sci Rep 7: 42571, 2017.
19. Kunk C, Kruger J, Mendoza G, Markitan J, Bias T, Mann A, Nath A, Geldenhuys WJ, Menze MA and Konkle ME: Mitoneet's reactivity of lys55 toward pyrooxidative phosphate demonstrations its activity as a transaminase enzyme. ACS Chem Biol 1: 2716-2722, 2022.
20. Colca JR, McDonald WG, Waldon DJ, Leone JW, Lull JM, Bannow CA, Lund ET and Mathews WR: Identification of a novel mitochondrial protein ('mitoNEET') cross linked specifically by a thiazolidinedione photoprobe. Am J Physical Endocrinol Metab 286: e252-e260, 2004.
21. Liu F, Dong Y, Zhong F, Guo H and Dong P: CISD1 is a breast cancer diagnostic biomarker associated with diabetes mellitus. Biomolecules 13: 37, 2022
22. Liang Y, Ye F, Xu C, Zou L, Hu Y, Hu J and Jiang H: A novel survival model based on a paradox related gene signature for predicting overall survival in bladder cancer. BMC Cancer 2: 943, 2021.
23. Yang J, Wei X, Hu F, Dong W and Sun L: Development and validation of a novel 3-gene diagnostic model for pancreatic adenocarcinoma based on ferrosis related genes. Cancer Cell Int 22: 21, 2022.
24. Wang H, Jia Y, Gu J, Chen O and Yue S: Iron death-related genes are involved in ashma and regulate the immune microenvironment. Front Pharmacol 14: 1087557, 2023.
25. Wu MN, Zhou DM, Jiang CY, Chen WW, Chen JC, Zou YM, Han T and Zhou LJ: Genetic analysis of potential biomarkers and therapeutic targets in ferroptosis from psoriasis. Front Immunol 13: 1104462, 2023.
26. Gao J, Dong M, Tian W, Xia J, Qian Y, Jiang Z, Chen Z and Shen Y: The role of CISD1 reduction in macrophages in promoting COPD development through M1 polarization and mitochondrial dysfunction. Eur J Med Res 29: 541, 2024.
27. Wu ZH, Tang Y, Yu H and Li HD: The role of ferroptosis in breast cancer patients: A comprehensive analysis. Cell Death Discov 7: 93, 2021.
28. Lu T, Li C, Xiang C, Gong Y, Peng W and Chen C: Overexpression of CISD1 predicts worse survival in hepatocarcinoma patients. Biomed Res Int 2022: 7823191, 2022.
29. Zang J, Cui M, Xiao L, Zhang J and Jing R: Overexpression of ferroptosis-related genes FSP1 and CISD1 is related to prognosis and tumor immune infiltration in gastric cancer. Clin Transl Oncol 25: 2532-2544, 2023.
30. Lei G, Zhuang L and Gan B: Targeting ferroptosis as a vulnerability in cancer. Nat Rev Cancer 22: 381-396, 2022.
31. Igarashi K, Shoji Y, Sekine Suzuki E, Ueno M, Matsumoto KI, Nakanishi I and Fukui K: Importance of locations of iron ions to elicit cytotoxicity induced by a fenton type reaction. Cancers (Basel) 14: 3642, 2022.
32. Searle AJ and Wilson RL: Stimulation of microscopic lipid peroxidation by iron and cysteine characterization and the role of free radios. Biochem J 21: 549-554, 1983.
33. Ploumi C, Kyriakakis E and Tavernarakis N: Coupling of autophagy and the mitochondrial intrinsic apoptosis pathway modulates proteostasis and ageing in Caenorhabditis elegans. Cell Death Dis 14: 110, 2023.
34. Hsiung KC, Tang HY, Cheng ML, Hung LM, Chin-Ming Tan B and Lo SJ: Mitochondrial bioenergetics deficiency in CISD-1 mutants is linked to AMPK-mediated lipid metabolism. Biomed J 7: 100806, 2024.
35. Furihata T, Takada S, Kakutani N, Maekawa S, Tsuda M, Matsumoto J, Mizushima W, Fukushima A, Yokota T, Enzan N, *et al*: Cardiac-specific loss of mitoNEET expression is linked with age-related heart failure. Commun Biol 4: 138, 2021.
36. Martinez A, Sanchez-Martinez A, Pickering JT, Twyning MJ, Terriente-Felix A, Chen PL, Chen CH and Whitworth AJ: Mitochondrial CISD1/CISD accumulation blocks mitophagy and genetic or pharmacological inhibition rescues neurodegenerative phenotypes in Pink1/parkin models. Mol Neurodegener 19: 12, 2024.
37. Ham SJ, Yoo H, Woo D, Lee DH, Park KS and Chung J: PINK1 and Parkin regulate IP3R-mediated ER calcium release. Nat Commun 14: 5202, 2023.
38. Zhang ZB, Xiong LL, Xue LL, Deng YP, Du RL, Hu Q, Xu Y, Yang SJ and Wang TH: MiR-127-3p targeting CISD1 regulates autophagy in hypoxic-ischemic cortex. Cell Death Dis 12: 279, 2021.
39. Tang CF, Ding H, Wu YQ, Miao ZA, Wang ZX, Wang WX, Pan Y and Kong LD: Gastrodin attenuates high fructose-induced sweet taste preference decrease by inhibiting hippocampal neural stem cell ferroptosis. J Adv Res: Sep 29, 2024 (Epub ahead of print).
40. Zhang X, Peng T, Li C, Ai C, Wang X, Lei X, Li G and Li T: Inhibition of CISD1 alleviates mitochondrial dysfunction and ferroptosis in mice with acute lung injury. Int Immunopharmacol 130: 111685, 2024.
41. Yang C, Yang Y, Hu X, Tang Q, Zhang J, Zhang P, Lu X, Xu J, Li S, Dong Z, *et al*: Loss of GCN5L1 exacerbates damage in alcoholic liver disease through ferroptosis activation. Liver Int 44: 1924-1936, 2024.
42. Dong W, Jiang Y, Yao Q, Xu M, Jin Y, Dong L, Li Z and Yu D: Inhibition of CISD1 attenuates cisplatin-induced hearing loss in mice via the PI3K and MAPK pathways. Biochem Pharmacol 223: 116132, 2024.
43. Geldenhuys WJ, Piktel D, Moore JC, Rellick SL, Meadows E, Pinti MV, Hollander JM, Ammer AG, Martin KH and Gibson LF: Loss of the redox mitochondrial protein mitoNEET leads to mitochondrial dysfunction in B-cell acute lymphoblastic leukemia. Free Radic Biol Med 175: 226-235, 2021.
44. Efimova I, Catanzaro E, Van der Meeren L, Turubanova VD, Hammad H, Mishchenko TA, Vedunova MV, Fimognari C, Bachert C, Coppieters F, *et al*: Vaccination with early atrophic cancer cells induce effective antitumor immunity. J Immunother Cancer 8: e001369, 2020.